LIP-STUDENTS-25-17

Probing Hadronic Interactions using the Earth's Magnetic Field

Elizabeth Osborne[1]

[1] *University of Liverpool, Liverpool, United Kingdom*

Project supervisor: Ruben Conceição, Bernado Tomé, Maria Amaral

October 5, 2025

Abstract. Ultra high energy cosmic rays produce extensive air showers once in contact with the Earth's atmosphere. The Pierre Auger Observatory uses a hybrid detector comprised of a surface detector and a fluorescence detector to analyse the secondary particles within these extensive air showers in order to provide an insight into the original high energy particle. In this project I utilised a simulator built on GEANT4 and ROOT software to simulate muon showers in order to better understand the hadronic interactions within the extensive air shower. I utilised the asymmetry azimuthal distribution to compare the implications of different variables on the number of muons detected at the ground as well as the signal detected with the Auger surface detectors. These variables included the simulated injection height of muons as well as different injection energies. This was all in the aim of building a stronger picture of the energy spectrum of the muons coming from the extensive air showers.

KEYWORDS: Ultra High Energy Cosmic Ray (UHECR), Extensive Air Shower (EAS)

1 Introduction

1.1 Ultra High Energy Cosmic Rays

Ultra-high-energy cosmic rays (UHECRs) are extremely energetic particles, typically ranging from protons to heavy nuclei such as iron, that originate from outside the Earth's atmosphere. The energies we are discussing are in the realm of 10^{18} – 10^{20} eV. These energies are substantially larger than anything we can detect or replicate on Earth, with the Large Hadron Collider (LHC) being able to reach energies of around 10^{12} eV. We are able to detect cosmic rays up to 10^{14} eV using balloon and satellite detectors, however the flux of particles beyond these energies is too infrequent to detect directly, and so we must study them indirectly through their extensive air showers.

1.2 Extensive Air Showers

Once the UHECRs reach the upper atmosphere they interact with the particles making up the atmosphere, causing cascades of particles directed towards the Earth, known as extensive air showers (EASs). The primary interaction goes on to cause a ripple effect of interactions through mostly hadronic and electromagnetic processes. An EAS has three components; electromagnetic, hadronic and muonic, with the hadronic component being the primary investigation of this project. Once the cascade of particles originating from the UHECR begins, many hadrons are generated in the process, an important one being charged pions. One of these pion's most frequent decay paths is to muons, muons have a long enough decay path that many can reach the ground, making them pinnacle in understanding the original hadronic interactions resulting from the UHECR.

1.3 Pierre Auger Observatory

The Pierre Auger Observatory is one of the world's leading detection sites to study the secondary particles from EASs caused by UHECRs. This observatory is located in Argentina and uses a combination of two types of detectors to create a hybrid detector [1].

The first type is the Surface Detector (SD), this is comprised of an array of water tanks which detects Cherenkov radiation produced inside. The water tanks are completely dark inside, except for when a secondary particle from a cosmic ray (CR) shower passes through the tank, then the interaction between the particle and the water produces an electromagnetic shock wave as the particle is travelling faster than the speed of light through the medium (water) – this is Cherenkov radiation. This electromagnetic shock wave is detected as a signal in the tank, we can then infer the particle's energy from said signal. There are around 1600 SD stations at the Pierre Auger Observatory, to maximise detection of these rare CR particles. As different water tanks detect different CR particles, we are also able to infer the EAS trajectory by analysing the time delay between detections, all to build a stronger picture of the EAS and hence of the UHECR.

The second type of detector is a fluorescence detector (FD), part of the EAS are charged particles which excite the nitrogen molecules in the atmosphere; the excited nitrogen produce fluorescence light in the UV range which can then be detected by the FD. The FD uses telescopes with large mirrors and photomultiplier tubes to observe the fluorescence light. There are 27 FD at Auger, the data collected at these telescopes can be used to indicate the energy of the primary UHECR as well as the maximum shower depth, in other words the depth into the atmosphere at which the shower has the most particles. However these detectors only work on clear, moonless nights in order to have the best visibility of the EAS, while the SD can operate constantly.

Implementing both the SD and FD as hybrid detectors allows for different elements of the EAS to be analysed. While the SD collects data on particle density at the ground, FDs allow us to analyse the EAS in the sky as it progresses. The unity of the two detectors together helps

to cross reference the energy data of the UHECR at both detectors, reinforcing the accuracy of the energy measurements.

1.4 Muon Puzzle

Monte Carlo simulations, for different hadronic interaction models, such as EPOS-LHC, QGSJetII-04 and SIBYLL-2.3d, as seen in figure 1 [2] below, simulate the muons from the EASs that are detected at the ground. However, there are large discrepancies in the number of muons that the simulations suggest are detected compared to the real data collected at the Pierre Auger Observatory – this is known as the muon puzzle [3]. These discrepancies can be as large as 30-60%.

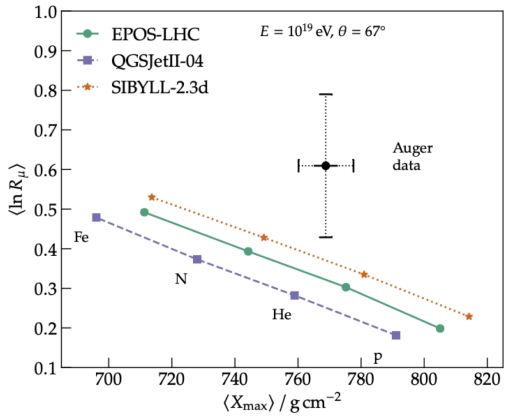

Figure 1. Average logarithmic muon content as a function of the average shower depth

In figure 1, we can see the number of muons produced at different maximum shower depths, as a result of various UHECRs, such as protons or iron. From all the simulations expressed, none of the data is anywhere near as large as the number of muons detected by Auger. The reasoning behind this disparity is thus far not understood, and so a better understanding of UHECRs is paramount.

2 Project Objective

Fundamentally, we are looking to characterise the cosmic ray, as explained, we do so by analysing the particles detected at the ground in order to understand the EASs. In this project, I primarily focused on simulating muon events at the detectors. I then looked at the distribution of these muon events with respect to their azimuthal angle, in order to gain a deeper understanding of how the EAS develops.

2.1 Shower Muon Distribution Universality

The distribution of the muon shower is not necessarily dependent on the primary cosmic ray. The shower can actually be characterised by three key components; the transverse momentum, the muon production depth and the energy. As we are looking at the muons, the electromagnetic portion of the shower seems immaterial. Thus, instead of having many parameters to analyse, we may merely assess these few 'universal' ones to understand EASs.

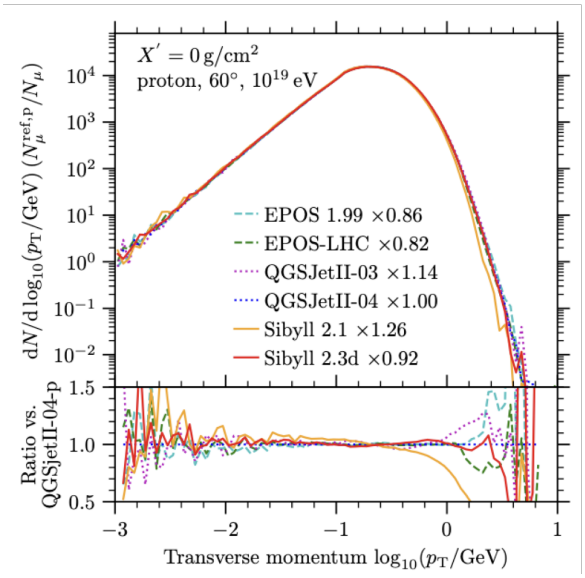

Figure 2. Particle Distribution with respect to Transverse Momentum

In figure 2, from [4], we can see how the transverse momentum of the shower compares to the distribution of particles. The transverse momentum is related to the lateral spread of the EAS, the number of particles gradually increases as you get closer to the centre of the shower, with a sharp decline after the peak P_T as the shower particles spread sideways.

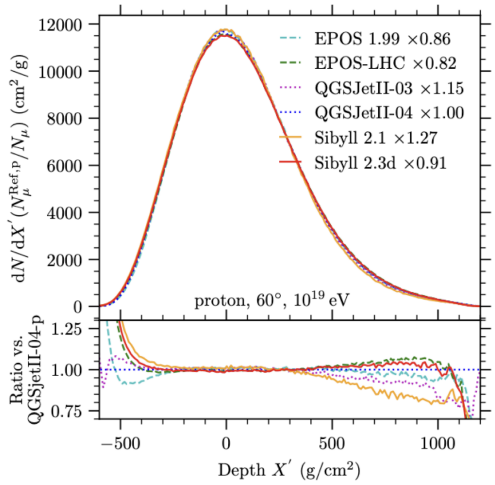

Figure 3. Particle Distribution with respect to Particle Production Depth

The second component to shower universality is the muon production depth, measured in g/cm^2, we can see, in figure 3 from [4], the muon distribution compared to its production depth. This quantity indicates how deep into the atmosphere the pion decayed to a muon, this gives

a longitudinal profile of the shower, as we can see it develop through the atmosphere. Looking at the plot, we see a steep incline in muons as the production depth reaches zero, in other words as the UHECR hits the atmosphere; then a steady decline as particles scatter and decay.

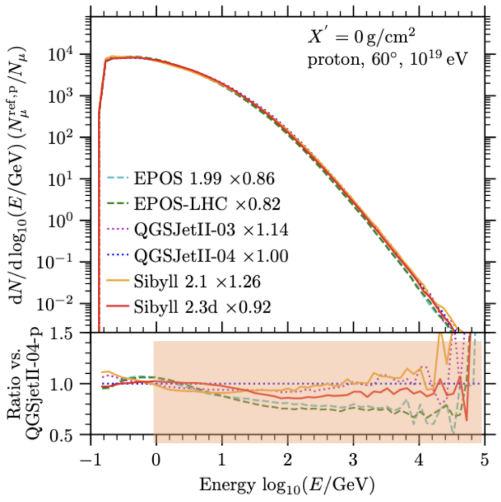

Figure 4. Particle Distribution with respect to Energy

The third defining component of the muon shower is the muons' energy spectrum. Figure 4, from [4], displays the energy spectrum of the muons, with a peak of muons at lower energies and fewer muons being detected at higher energies.

Checking the transverse momentum, muon production depth and energy spectrum through a variety of simulations we see very little discrepancy, we see the robustness of these three components in characterising the muon shower. The only visible differences across models arise only for the muon energy spectrum for muons with energies greater than 1 GeV.

2.2 Inclined Shower Events Footprint

The footprint and distribution of the muons detected at the ground will heavily depend on the geometry of the shower. Figure 5 below, from [5], is the framework used to extrapolate this geometry.

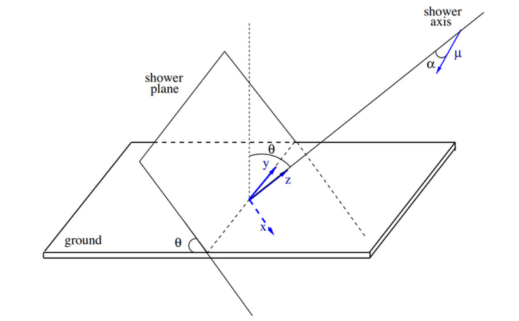

Figure 5. Shower Plane Geometry

The muon travels towards the ground at an angle α relative to the shower axis. Instead of studying the footprint directly at the ground, we take the footprint in the shower plane, perpendicular to the shower axis. Depending on the zenith angle θ, the angle between the vertical and the shower axis, we can get drastically different muon footprint distributions, as seen in figures 6 and 7, both from [5].

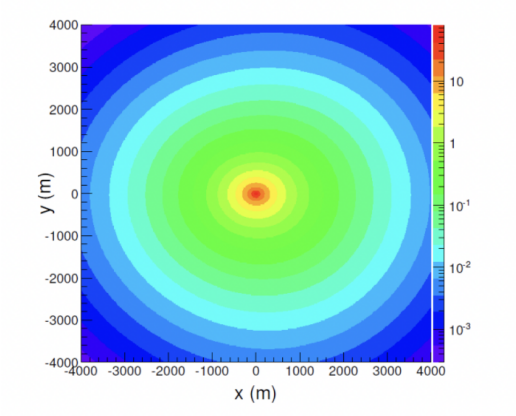

Figure 6. Shower Footprint at $\theta = 70°$

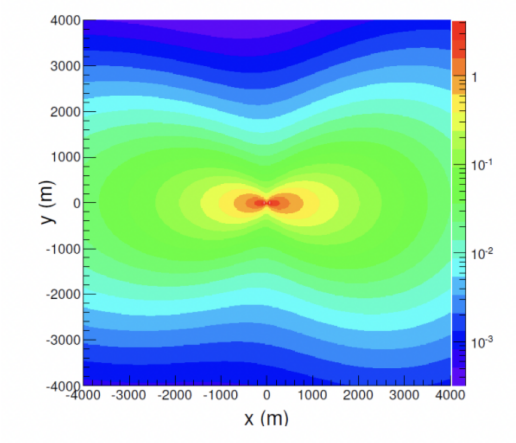

Figure 7. Shower Footprint at $\theta = 84°$

This difference in footprint can be attributed to the Earth's magnetic field. At a zenith angle of 80° the shower axis, and so the incoming muon, is less inclined than that at 70°, and so the incoming muons interact more with the Earth's magnetic field. Therefore, the steepness of the muon's trajectory influences how much the Earth's magnetic field bends the muon, affecting the muon's probability of reaching the ground, or whether its will be directed back towards space, all demonstrating the shower muon footprint's sensitivity to the Earth's B field.

2.3 Measurement of the Muon Energy Spectrum through the Inclined Shower Footprint

In order to closer analyse the Muon Energy Spectrum, I implemented the muon azimuthal distribution. This contained two key variables, the azimuthal angle ϕ and the distance from the event to the centre of the shower footprint.

$$\phi = \arctan\left(\frac{Y_{\mathrm{sh}}}{X_{\mathrm{sh}}}\right) \tag{1}$$

The azimuthal angle is the angle between the positive y-axis on the shower plane, denoted by Y_{sh} in equation 1, and the negative x-axis, X_{sh}.

$$r = \sqrt{{X_{\mathrm{sh}}}^2 + {Y_{\mathrm{sh}}}^2} \tag{2}$$

The distance from the detected event to the shower footprint centre was calculated as shown in equation 2 and denoted by r. These two variables together define the distribution of the muon footprint.

This distribution is called the event asymmetry azimuthal distribution, and is denoted by A_N.

$$A_N = \sum_j r_j n_j(\phi, r_j) \tag{3}$$

Each event, n_j, with specific polar coordinates, is then weighted by the distance between the event and the shower centre. This distribution is plotted for each azimuthal angle. The inclination of the shower means the footprint is no longer symmetrical in the azimuth and so introduces the dependence on the azimuthal angle.

3 Simulation Framework

3.1 MuonTracker

To run the simulations, I used the project titled MuonTracker, which uses GEANT4 software to simulate the muons detected at the Pierre Auger Observatory. After running the simulations using GEANT4 software, the data is then saved and analysed using ROOT, I was then able to use the root files in python to analyse and plot the distributions.

Through using GEANT4, I was able to build complex simulations, implementing multiple particle processes. I was able to isolate these different processes, including multiple and Coulomb scattering, electromagnetic and decay processes, as well as being able to simulate the atmosphere being 'on' and so present, or 'off'. Furthermore, it gave me the ability to apply various values for the Earth's magnetic field, all of which were in the aim to fully simulate and analyse how the muons from the EASs behave.

3.2 Simulations performed

In order to simulate the muons being detected at Auger, I simulated a variety of muon showers with different variables changed. I ran simulations at 5 km, 7.5 km, 10 km, 12.5 km and 15 km muon injection heights to see how the azimuthal distribution varied. I then also simulated 10 GeV, 100 GeV and 1 TeV muon injection energies to see how the distribution changed between comparatively low and high energy muons. Through all these simulations, I had the atmosphere 'on' with all scattering, electromagnetic and decay processes activated. I also set the magnetic field to $\vec{B} = (2.58664\times10^{-6}, 19.85244\times10^{-6}, -14.1\times10^{-6})$ T as this magnetic field configuration produced the largest separation between positive and negative muons as outlined in [5].

4 Results

4.1 Assessment of Shower Footprint Azimuthal Asymmetry through A_N

I first looked to assess the Azimuthal asymmetry distribution of the number of muons at varied azimuthal angles. In order to further inspect the muon energy spectrum, I looked to analyse two muon injection energies, 10 GeV and 100 GeV.

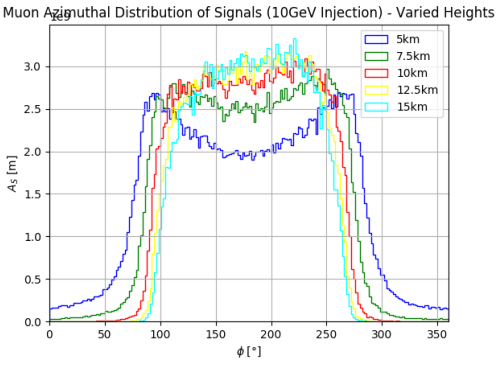

Figure 8. Muon Azimuthal Distribution for 10 GeV muons at varied injection heights

In figure 8, it can be seen that different injection heights each follow a distinct shape. This is due to the fact that at lower energies, like 10 GeV, scattering and decay processes play a much larger role in the number of muons reaching the ground.

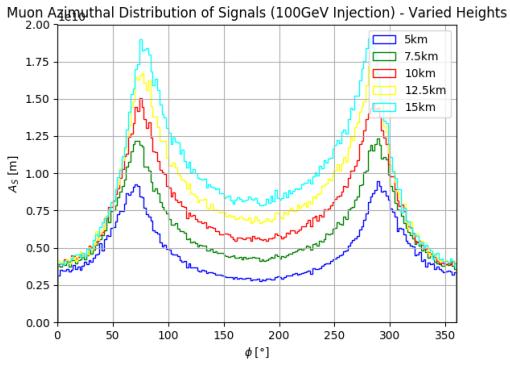

Figure 9. Muon Azimuthal Distribution for 100 GeV muons at varied injection heights

Whilst for higher muon energies, such as 100 GeV displayed in figure 9, the azimuthal distribution at different heights all follow a similarly shaped distribution. At higher energies, the muons have a long decay length, thus over distances 5-15 km the shape of the distributions remain essentially unaltered.

Figures 8 and 9, demonstrate the robustness and susceptibility of the muon energy spectrum, with different simulated injection energies we get vastly different distribution shapes. This is what I wish to further explore.

4.2 Check A_N contributions (different particles)

I next had to consider the possibility that the data detected at the ground at Pierre Auger is not necessarily the number of muons. The SD detects a signal when a particle passes through the tank, we cannot yet assume all these signals are as a result of muons. We must take into account other secondary particles reaching the ground, such as electrons and positrons.

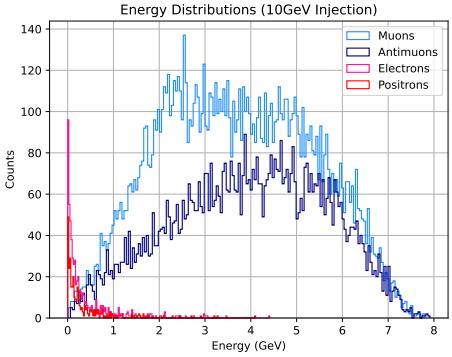

Figure 10. Particle Energy Distribution for a 10 GeV Injection

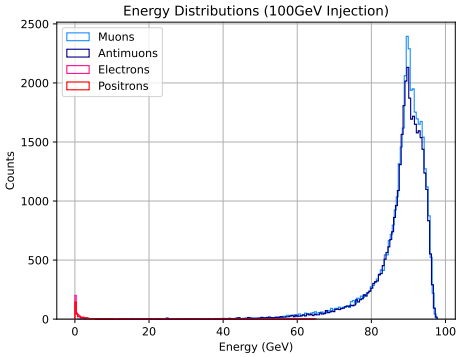

Figure 11. Particle Energy Distribution for a 100 GeV Injection

As a result of this, I then looked to compare the simulated detections depending on the simulated particle type. It can be seen in figures 10 and 11 that at both 10 GeV and 100 GeV injections the contribution of possible other particles such as electrons and positrons is negligible, with the majority of them having little to no energy. This strongly indicates that the signal received in the water tanks can be interpreted as originating from the muons in the EAS.

4.3 Check A_N vs. A_S

After corroborating that the detected signal in the tank may be interpreted as the muons hitting the ground, I began to explore the azimuthal asymmetry of the signal received in the SDs as opposed to the asymmetry of the muon events as before. For this I had to revise my distribution equation as so in equation 4 below.

$$A_S = \sum_j r_j S(\phi, r_j) \tag{4}$$

Analysing the overall simulated signal brought me closer to revealing the realistic energy spectrum that detected data represents at Auger.

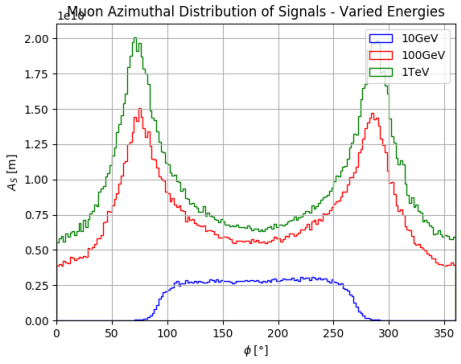

Figure 12. Azimuthal Distribution of the Detected Signal for varied Injection Energies

In figure 12, I plotted the signal asymmetry for low and high energies, namely 10 GeV, 100 GeV and 1 TeV. It can

be seen that the distribution of signals at 10 GeV varies drastically in shape and size to the higher energies of 100 GeV and 1 TeV.

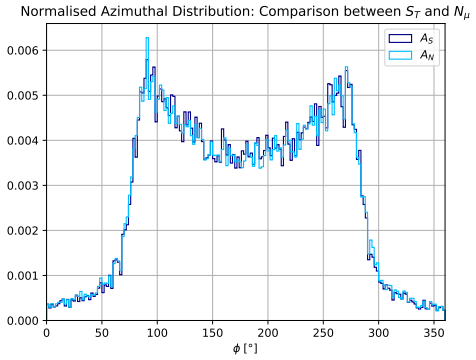

Figure 13. A Comparison of the Signal Asymmetry and the Event Asymmetry at a simulated injection energy of 10 GeV

In figure 13, I then proceeded to plot the azimuthal distribution of the signal asymmetry along with the event asymmetry at 10 GeV specifically to have a direct comparison of the two plots, with 10 GeV seemingly to be the most sensitive injection energy. The signal asymmetry distribution and the muon event asymmetry distribution barely deviate from each other, and so this plot coupled with the energy distributions in figures 10 and 11, I contended that the muons from the EAS can account for the signal detected at Auger.

I finally wanted to analyse the sensitivity of the asymmetry distribution to the muon energy spectrum. I plotted the distribution of the three energy signal asymmetry, rather than muon event asymmetry, azimuthal distributions summed and weighted according to the energy spectrum in figure 5, as outlined in [5]. I increased the weight of the 10 GeV energy distribution by a small amount, 10%, in order to analyse the sensitivity of the footprint to slight changes to the muon energy spectrum.

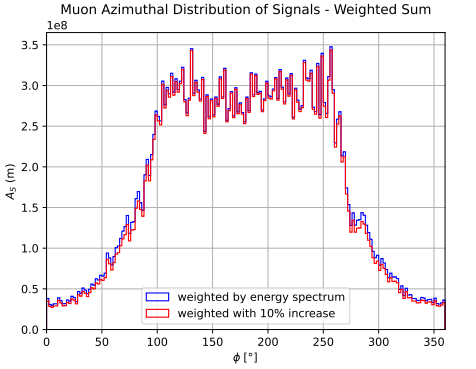

Figure 14. A comparison of the summed energies 10 GeV, 100 GeV and 1 TeV for the Signal Asymmetry and the Event Asymmetry, with a 10% increase in the 10 GeV energy

As can be seen in figure 14, this tiny increase in weight had a noticeable effect on the distribution. Specifically at $\phi \sim 80°$ and $\phi \sim 290°$, there is a discernible difference between the two distributions. This visible effect on the shower footprint implies the possibility to more accurately measure muon EAS energies at the Pier Auger Observatory in the future.

5 Conclusions

This project set out to investigate UHECRs, as these particles are of too high an energy to analyse directly, indirect methods must be implemented, through studying its EAS and the secondary particles which accumulate. This was all in the aim of understanding these UHECR more precisely. It became clear, through the understanding of hadronic interactions within the EAS, that muons were the key to this.

Through the application of the real findings and research being undertaken at the Pierre Auger Observatory and the use of GEANT4 and ROOT software, I simulated realistic runs of muon showers which could be detected at Auger. I analysed the different variables which implicate the muon shower footprint being detected at the ground, such as muon injection heights and muon injection energies. This was all in the aim of further understanding the sensitivity of the muon shower footprint to the muon energy spectrum.

However, in order to compare my simulated data with the data at Auger, I had to take into account the signal received from the Cherenkov radiation in the water tanks. As this may be a result of muons or electrons/positrons. The counts of simulated energies, isolating the types of particle, revealed muons and anti-muons were the particles with significant energy at the ground. A further comparison of the total signal asymmetry against the muon event asymmetry revealed the two distributions are incredibly similar, cementing the idea that the signal being detected at the tank is predominantly a result of incoming muons from the EASs.

Ultimately, after consolidating the origin of the signal, I inspected the signal sensitivity to slight changes in energy. Summing all the energy distributions and weighting them accordingly, I then increased the weight of the 10 GeV simulation by a mere 10% to explore the aforementioned sensitivity of the shower footprint to the muon energy spectrum. This revealed slight but notable deviations between the two distributions, implying a strong possibility to further analyse the muon EAS energies at the Pierre Auger Observatory.

Acknowledgements

A special thank you to Ruben Conceição, Bernado Tomé and Maria Amaral for all their help and guidance throughout this project.

References

[1] Nuclear Instruments and Methods in Physics Research Section A: Accelerators, Spectrometers, Detectors and Associated Equipment **798**, 172 (2015)

[2] A. Aab, P. Abreu, M. Aglietta, J. Albury, I. Allekotte, A. Almela, J. Alvarez-Muñiz, R. Alves Batista, G. Anastasi, L. Anchordoqui et al., Physical Review Letters **126** (2021)

[3] J. Albrecht, L. Cazon, H. Dembinski, A. Fedynitch, K.H. Kampert, T. Pierog, W. Rhode, D. Soldin, B. Spaan, R. Ulrich et al., Astrophysics and Space Science **367** (2022)

[4] R. Conceição, P. Assis, P. Costa, M. Freitas, B.S. González, B. Tomé, *Innovative Approaches to Unravel the Shower Components' Energy Spectrum with a Single Hybrid Station*, in *Proceedings of 39th International Cosmic Ray Conference — PoS(ICRC2025)* (2025), Vol. 501, p. 225

[5] P.A.D.B. Tomé, Master's thesis (2025)